
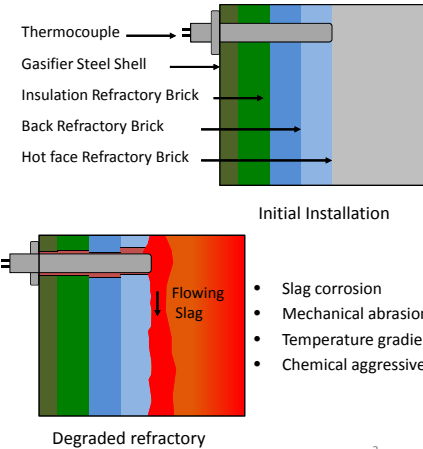


In-situ Acoustic Measurements to Temperature Profile in Extreme Environments

Yunlu Jia and Mikhail Skliar



Refractory Degradation




Stage	Sample	Description
1		New • Refractory may contain internal cracks from pressing, firing.
2		Preheat • Preheat spalling due to hoop stresses.
3		Infiltration, Corrosion • Molten slag penetration on hot face, cracks and pores. • Surface corrosion due to slag begets.
4		Horizontal Crack Formation due to: • Thermal cycling • Stress accumulation • Creep
5		Void Formation • Cracks join • Internal void formation • Spalling (spalling begins) • Creep occurs on slag penetrated hot face • Hot face corrosion continues
6		Renewed Cycle • Material breakdown on hot face • Steps 1-6 repeat

- Slag corrosion
- Mechanical abrasion
- Temperature gradient
- Chemical aggressiveness


2 Stages of refractory degradation [1].

Direct Temperature Measurement


- Develop hardened sensors that can withstand harsh environment for long time.
 - Heavy sheathing makes such devices less sensitive to dynamic changes in temperatures, which are important in the refractory life management since rapid temperature variations can introduce thermal stresses.




Thermocouple protection system for gasifier application.



Rosemount Sapphire TC





NETL-USDOE

Prof. Zhang Jiansheng: "Domestic TC survive ~1-2 weeks; Rosemount sapphire TC: ~4-6 weeks"

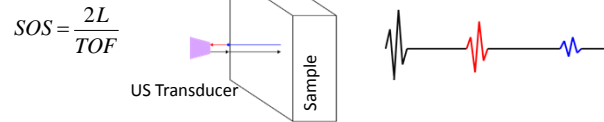
Other temperature measurements

- *Indirect (secondary) measurements* that are easy to obtain (T , P and compositions of in/out streams) are used with appropriate models to *infer* otherwise inaccessible operating parameters inside the reactor zone and the state of the refractory.
 - Few examples in gasification: reactor temperature reported in ppm of methane -- Tampa Electric IGCC Demonstration Project [3]. Economically appealing option.
 - Quality of inferences is affected by modeling errors and uncertainties.
 - Measurement accuracy, sensitivity, and response time compare poorly with direct measurements.
- **Optical measurement:**
 - Infrared window required to maintain pressure boundary
 - Deposition of slag & other contaminants blocks sight path
- **Acoustic Pyrometer:**
 - Sensitive to surroundings
 - Spatial resolution limited by low acoustic frequency

4

Acoustic Temperature Measurements

- Speed of sound (SOS) is temperature dependent in gases, liquids, and solids. SOS can be obtained by measuring time of flight (TOF) of the test pulse:



- Key difficulty:** *When temperature changes along the path of US propagation*, the acoustic TOF measurements depend on temperature distribution in a complex way:

$$TOF = \int_n^{r_c} \frac{2}{f(T(t,r))} dr$$

- Key uncertainty:** *How strong is SOS vs. T dependence?*
 - The answer to this question determines **achievable accuracy** of temperature measurements.

5

Estimating temperature distribution from TOF measurements

- Experimentally establish the relationship between T and SOS/TOF and identify the function $f(\cdot)$:

$$TOF = \int_n^{r_c} \frac{2}{f(T(t,r))} dr$$

A small diagram of a sample block and a pulse waveform is shown to the right of the equation, mirroring the diagram in slide 5.

- Use the result and the heat transfer model

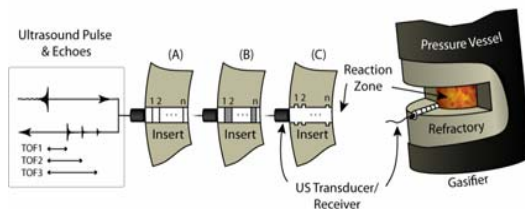
$$\rho C \frac{\partial T}{\partial t} = k \frac{1}{r} \frac{\partial}{\partial r} \left(r \frac{\partial}{\partial r} \right) T$$

to *estimate* the temperature distribution

6

Direct Ultrasound (US) Measurements of Temperature Distribution

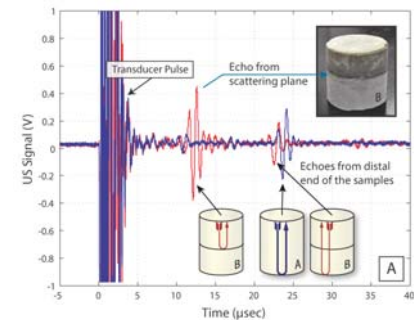
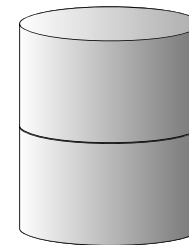
- Create multiple partial reflections that give information about temperature distribution in different segments of the refractory.
 - The ability to create partial internal reflections and their spacing determines **achievable spatial resolution**.



- Methods to create partial reflections:
 - Scatters;
 - Change in US impedance;
 - Change in geometry

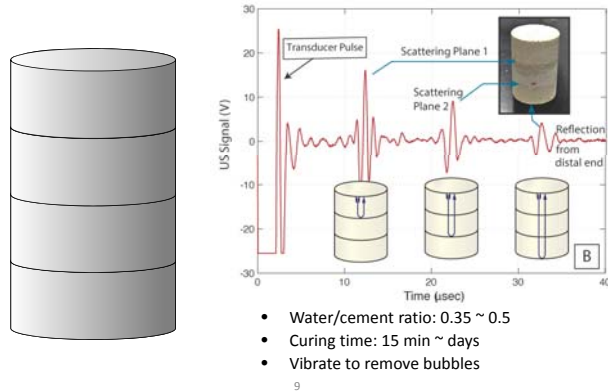
7

A: Steel shots were embedded as ultrasound scatters to produce partial reflection at the midpoint of ultrasound propagation path

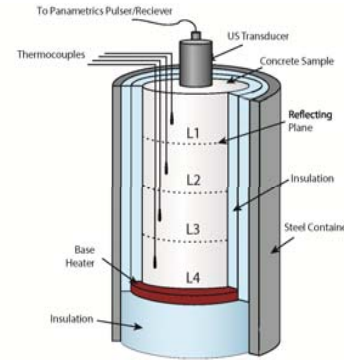


8

B: Two internal interfaces obtained by sequentially casting three layer of identical formulation and allowing for a partial curing before casting the next layer



Non-uniform Temperature Distribution Experimental Setup



- Heated at the base
- Surface temperature measured by TCs
- Experiments repeated least 6 times to calculate 95% CI

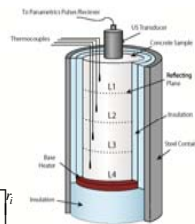
10

Piecewise Linear Temperature Distribution

- Assume linear distribution in different segments. Slopes and intercepts may be different but temperature must be continuous
- Linear relationship between the SOS and temperature T found from calibration data
- TOF for each layer:

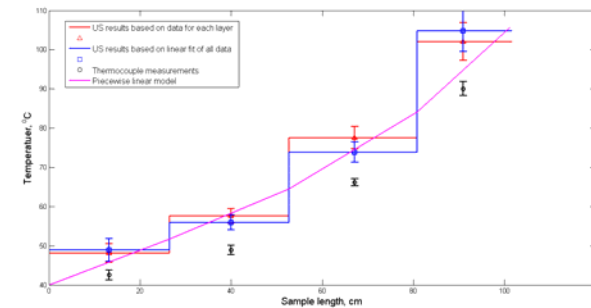
$$TOF_i - TOF_{i-1} = \int_{r_{i-1}}^{r_i} \frac{2}{a(m_i r + n_i) + b} dr$$

$$= \frac{2}{a m_{i-1}} \ln \left[a(m_{i-1} r + (m_{i-1} - m_i) r_{i-1} + n_{i-1}) + b \right]_{r_{i-1}}^{r_i}$$



11

Results



- Accurate estimation of the temperature distribution strongly depends on the assumptions about the shape of that distribution and the method used to interpret the measurements of the ultrasound TOF

12

Algorithm for finding distribution that satisfies thermal model

- Predict temperature by solving

$$\rho C \frac{\partial T}{\partial t} = k \frac{1}{r} \frac{\partial}{\partial r} \left(r \frac{\partial T}{\partial r} \right)$$

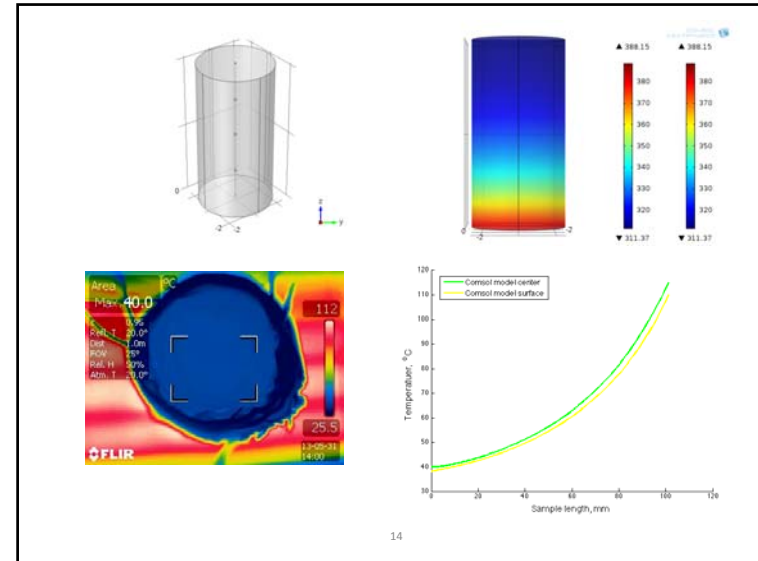
with boundary conditions:

- Cold/hot side temperature provide by TC and thermal camera
- Heat loss through the sides equal

$$q = h(T_a - T)$$

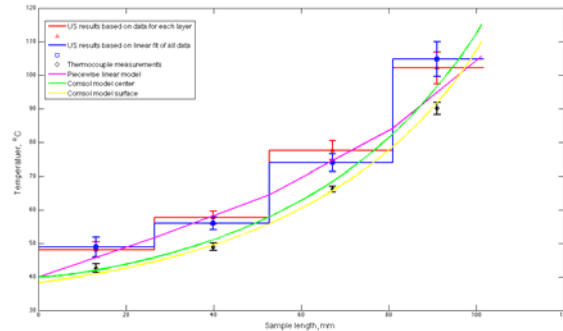
- Calculate the corresponding TOF using SOS vs. T calibration curve
- Compare predicted TOF with measurements
- Adjust h to improve fit

13



14

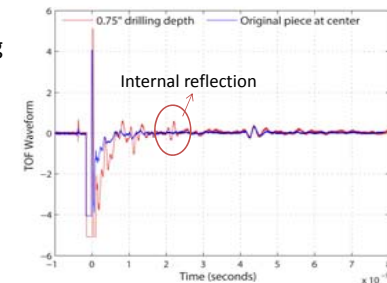
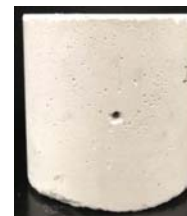
Temperature Distributions Obtained Based on US Measurements, Thermal Model and Consol Model are Compared with TC Measurements



15

Engineering Refractory with Partial Internal Reflections

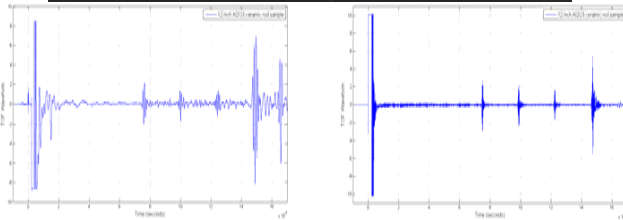
- Tested in castable and pre-cast, pressure formed, machinable alumina ceramics: max temperature 3000°F
- 2" I.D. and 2" height sample
- 1/16" I.D. carbide drill bit
- US tested with 1/4" drilling depth



16

High Temperature Refractory Model

- Partial echoes from 3 holes at 2, 4, and 6" from the hot end of 1" x 12" Al₂O₃ rod plus complete US reflection from hot end
- 5MHz central frequency was selected

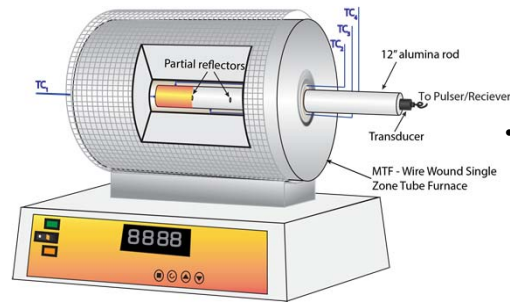


(a) 1MHz V603

17

(b) 5MHz V609

High Temperature SOS vs. Temperature Calibration Curve Experimental Setup



- Surface temperature measured by OMEGA® Nextel Ceramic Insulated TCs (rated to 1200°C for continuous use)

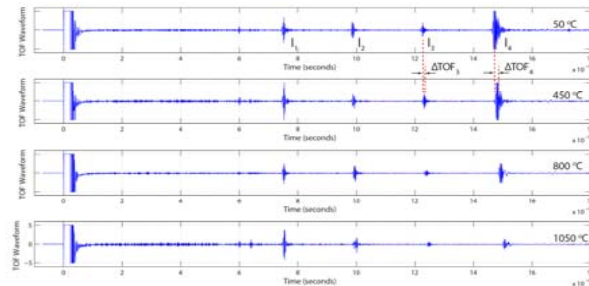
- Heated inside tube furnaces (maximum operating temperatures 1200°C)
- Temperatures changed in 50°C increments, from 50 to 1150°C
- US measurement between I3 and I4 (marked red) was used for SOS vs. temperature calibration curve

18

SOS Calculation

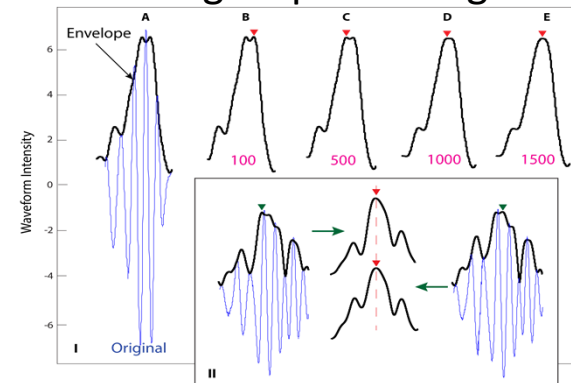
- Cross-correlation b/w echoes gives change in TOF and SOS(T)

$$SOS(T) = \frac{2(I_4 - I_3)}{TOF_{ref} + (\Delta TOF_4 - \Delta TOF_3)_T}$$



$I_4 - I_3$ was measured by micrometer at room T and corrected for thermal expansion at different temperatures

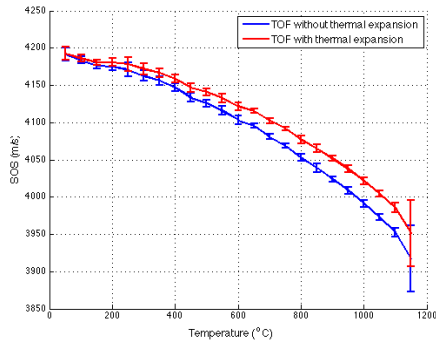
Signal processing



- Accurate and robust timing of ultrasound echoes
 - Cross-correlation of waveform envelope: reduces effect of broadening
 - Filtering by anisotropic diffusion: reduces influence of changing waveform features

20

High Temperature SOS vs. Temperature Calibration Curve

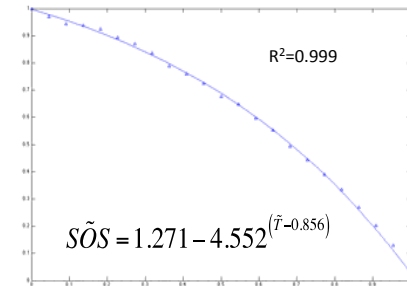


- Thermal expansion corrections are included
- Strong dependence on temperature
- The highest errors from 1150°C is less than 1.3%
- 65% measured temperatures have accuracy with $\pm 1^\circ\text{C}$

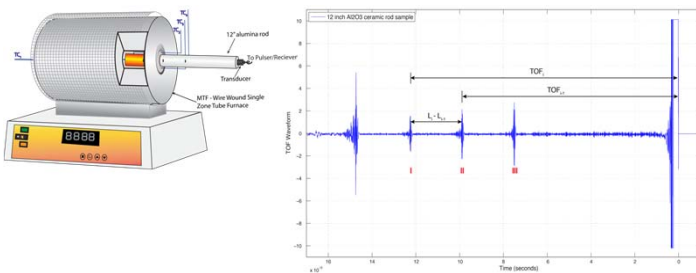
Calibration Curve Model

- In steel, for every 100°F in T increase, SOS decreases by 1%
- Fit SOS vs. T to equal percentage model:

$$S\tilde{O}S = a - R^{(\tilde{T}-b)} \quad \text{where} \quad s\tilde{O}S = \frac{SOS - SOS_{\min}}{SOS_{\max} - SOS_{\min}} \quad \text{and} \quad \tilde{T} = \frac{T - T_{\min}}{T_{\max} - T_{\min}}$$



High Temperature Experiments



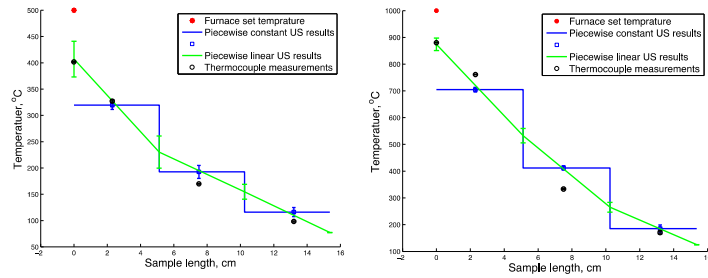
- Alumina rod is partially inserted into the furnace
- TCs provide independent measurements
- Measurements of TOF and the SOS vs. temperature calibration curve were used to find the temperature distribution

Assumptions on Temperature Distribution

- Piecewise constant temperature in each segment
- Temperature changes linearly, but with different slopes
- Two experiments: Furnace temperature set to 500 and 1000°C
- US measurements at steady state temperatures

$$TOF_i(T) - TOF_{i-1}(T) = \frac{2(L_i(T) - L_{i-1}(T))}{SOS_i(T)}$$

Distributions under Different Assumption: Comparison with TC Measurements

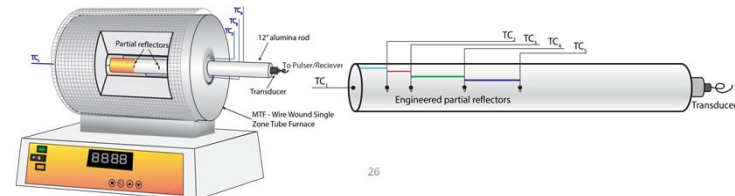


- Piecewise linear distribution better agrees with TC measurements
- Good agreement between US and TC measurements!

25

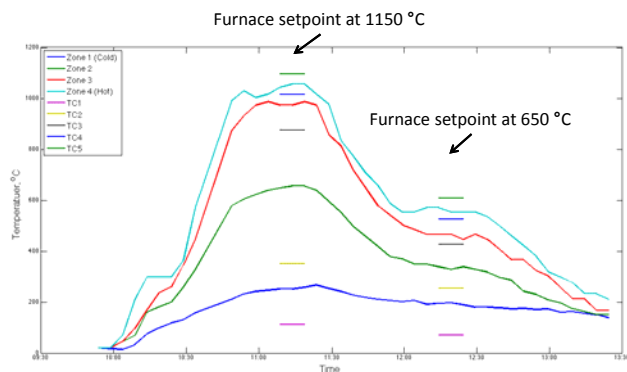
Time-dependent measurements

- Refractory rod was partially inside furnace and partially exposed to ambient T
- Piecewise constant assumption
 - Temperature in each segment is constant
- Furnace temperature set at 1150°C
 - Initially, at room temperature
 - After reaching steady state, sample was cooled inside the furnace
- TCs provided independent measurements at steady state only



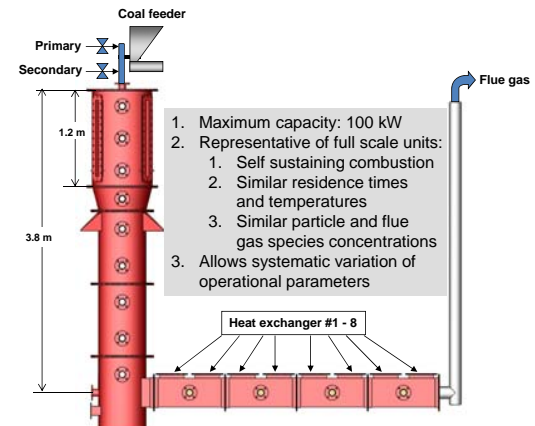
26

Time-dependent results

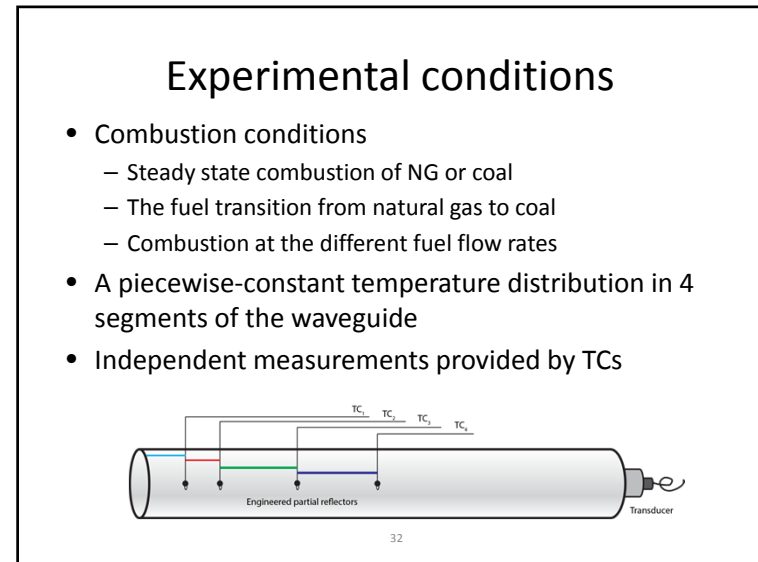
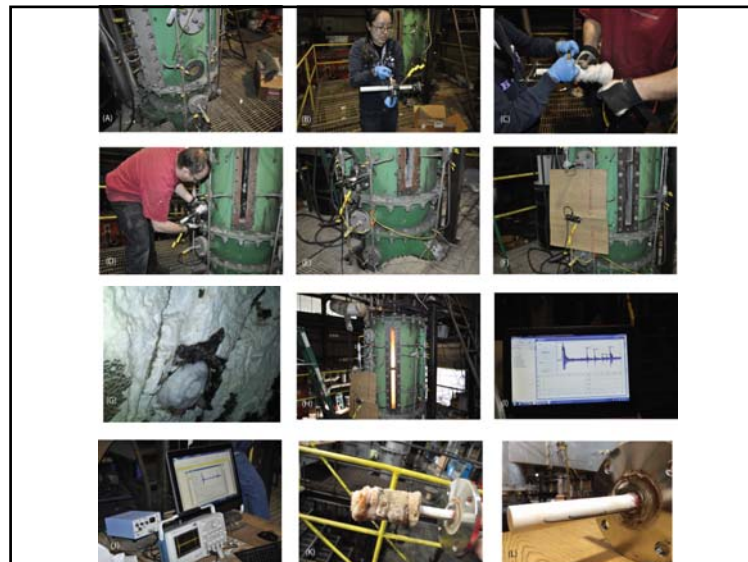
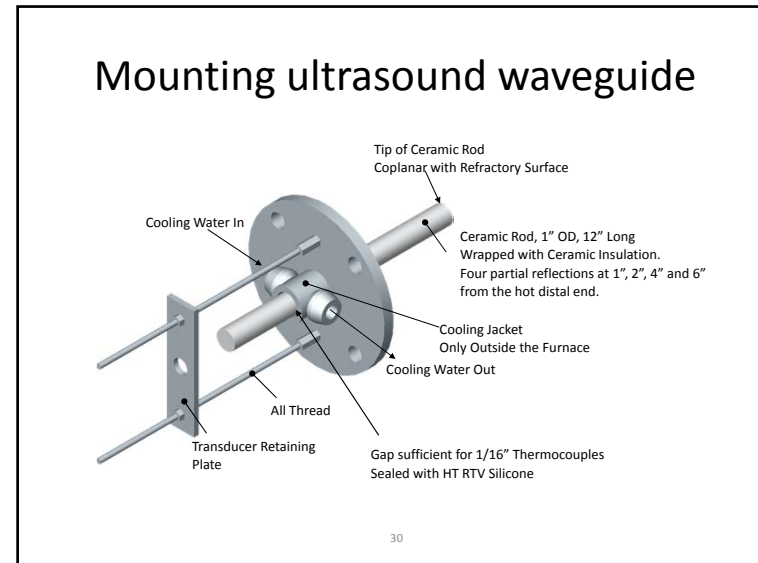
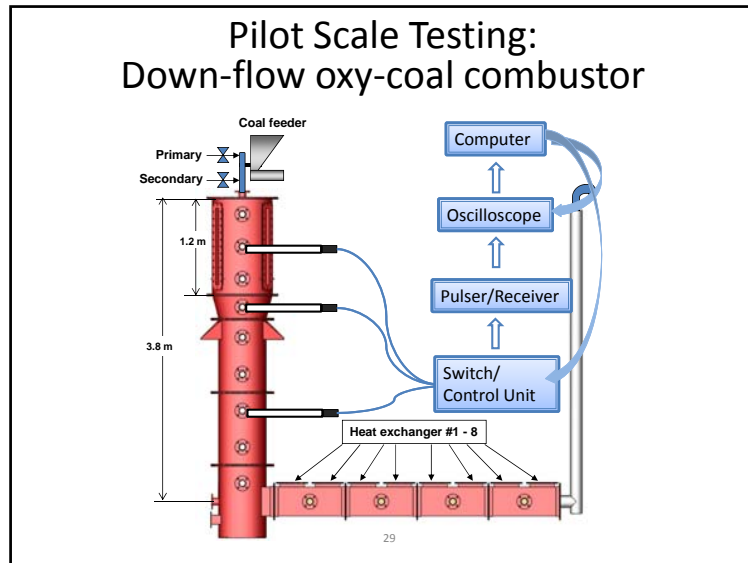


27

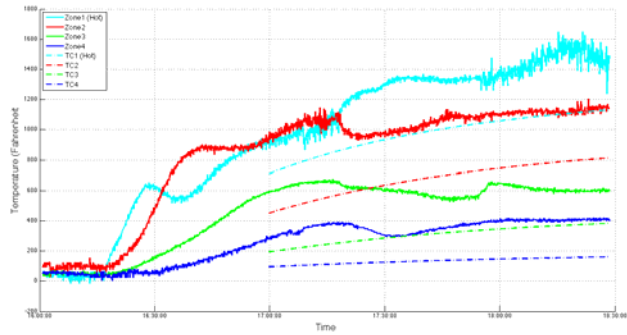
Pilot Scale Testing: Down-flow oxy-coal combustor



28

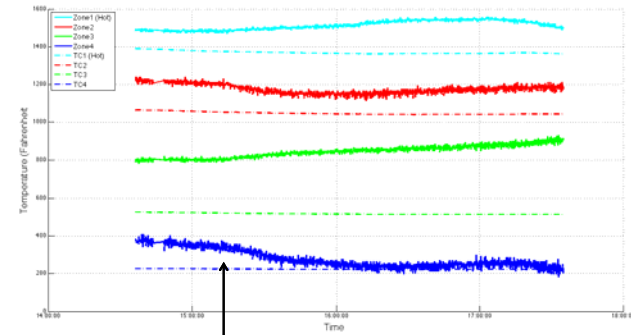


Natural gas preheating



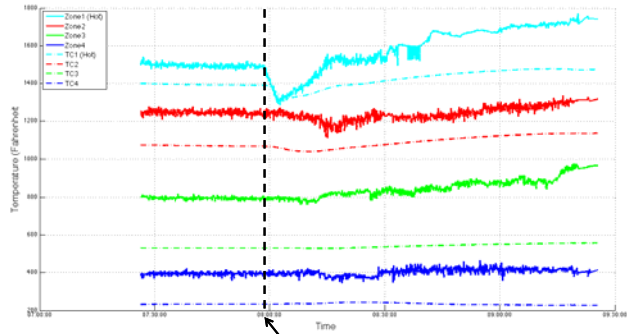
33

Stable natural gas combustion



34

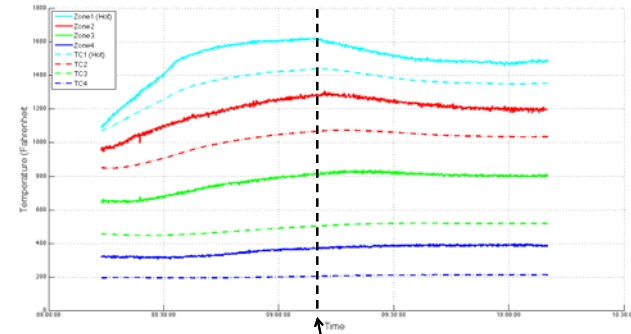
Transition from natural gas to coal combustion



Changed fuel from natural gas to coal

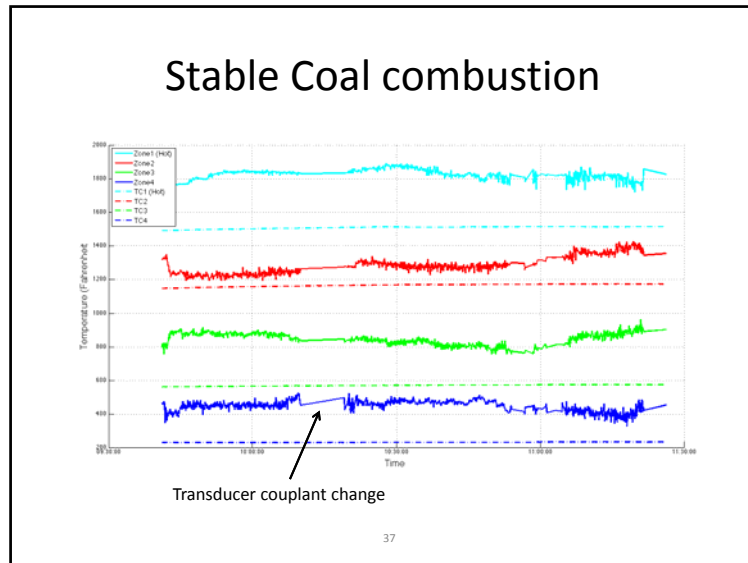
35

Coal combustion with coal feed rate adjusted





Reduced coal feed rate

36



After tests

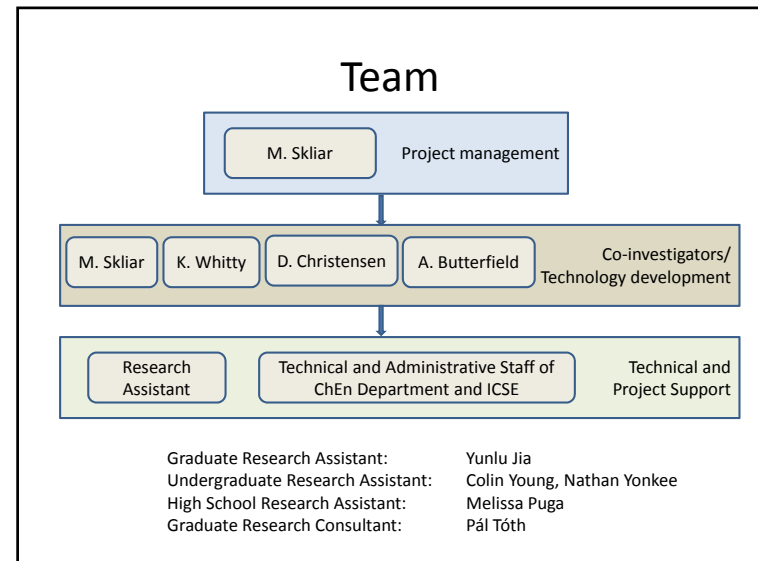



(Left) Ash deposition found on the ceramic insulation that covered the alumina rod. (Right) The alumina rod appears visually undamaged after the pilot scale test.

- Revealed issues
 - Continuous real-time monitoring will require permanent coupling between the transducer/receiver and the waveguide
 - Significant deterioration of the ultrasound signal was observed after long time operation at high temperatures

38

- ### Conclusions
- Noninvasive ultrasound measurements of temperature are possible, as demonstrated in the lab and at pilot scale
 - SOS dependence on temperature is sufficiently strong to allow for accurate measurements of temperature distribution
 - During pilot testing, all relevant process changes were captured in real time
 - Different waveguide materials should be selected for continuous high temperatures operation
 - Signal processing and data interpretation algorithms should be further optimized
 - Method can be used with existing units. New units can be designed to measure T distribution in multiple locations
 - Broadly applicable in other energy applications
 - Can be used to measure temperature distribution on a line, surface, or volume



Acknowledgements

- Funding by the U.S. Department of Energy National Energy Technology Laboratory, Grant DEFG2611FE0006947.
- Project manager: Barbara Carney

41



References

1. Bennett, J.P., Kyei-Sing, K., "Refractory Liner Materials used in Slagging Gasifiers," *Refractory Applications and News*, 9: 20-25, 2004.
2. Dogan, C.P., Kwong, K.-S., Bennett, J.P. and Chinn, R.E. "Improved Refractories for Slagging Gasifiers in IGCC Power Systems", DOE Report 835687.
3. Hornick, M.J. McDaniel, J.E., "Tampa Electric Integrated Gasification Combined-Cycle Project," Final technical report for project under Cooperative Agreement DE-FC-21-91MC27363, 2002.
4. Liu, J.T.C., Rieker, G.B., Jeffries, J.B., Hanson, R.K., Gruber, M.R., Carter, C.D. and Mathur, T., "Near infrared Diode Laser Absorption Diagnostic for Temperature and Water Vapor in a Scramjet Combustor," *Applied Optics*, 44: 6701-6711, 2006.
5. Muzio L.J., Eskinazi, D., Green, S., "Acoustic pyrometry: new boiler diagnostic tool," *J. Power Engineering*, 12:32-37, 1989.
6. Green, S.F., "An acoustic technique for rapid temperature distribution measurements," *J. Acoustical Society of America*, 77: 765-769, 1985.
7. Bramanti, M., Tonazzini, A., Tonazzini, A., "An acoustic pyrometer system for tomographic thermal imaging in power plant boilers," *IEEE Trans. Instrumentation and Measurement*, 45:87-94, 1996.
8. Lu, J., Takahashi, S., Takahashi, S., "Acoustic computer tomographic pyrometry for two-dimensional measurement of gases taking into account the effect of refraction of sound wave paths," *Measurement Science and Technology*, 11: 692-697, 2000.
9. Lee, Y.J., Khuri-Yakub, B.T., Saraswat, K., "Temperature measurement in rapid thermal processing using the acoustic temperature sensor," *IEEE Trans. Semiconductor Manufacturing*, 9: 115-121, 1996.
10. Arthur, R.M., Trobaugh, J.V., Straube, W.L., Moros, E.G., "Temperature dependence of ultrasonic backscattered energy in motion compensated images," *IEEE Trans. Ultrasonics, Ferroelectric and Frequency Control*, 52:1644 – 1652, 2005.
11. M. Skliar, K. Whitty, and A. Butterfield, "Ultrasonic temperature measurement device," PCT patent application, Pub. No: WO/2011/088393, International Application No: PCT/US2011/021396, 2011.
12. Y. Jia and M. Skliar, "Ultrasound measurements of temperature profile across gasifier refractories," Proposal to present at the Annual AIChE Meeting, November, 2012.
13. Y. Jia, Melissa Puga, A. Butterfield, D. Christensen, K. Whitty, and M. Skliar "Ultrasound Measurements of Temperature Profile Across Gasifier Refractories: Method and Initial Validation," *Energy Fuels*, Article ASAP, DOI: 10.1021/ef3021206, 2013.

42

Thank you!

43

